HHS Public Access

Author manuscript

Biochem Pharmacol. Author manuscript; available in PMC 2016 November 22.

Published in final edited form as:

Biochem Pharmacol. 2016 March 1; 103: 109–117. doi:10.1016/j.bcp.2016.02.004.

Copper and protons directly activate the zinc-activated channel

Sarah M. Trattnig[a,b], **Agnes Gasiorek**[a,b], **Tarek Z. Deeb**[a], **Eydith J. Comenencia Ortiz**[a], **Stephen J. Moss**[a], **Anders A. Jensen**[b], and **Paul A. Davies**[a,*]

[a]Department of Neuroscience, Tufts University School of Medicine, Boston, MA 02111, USA

[b]Department of Drug Design and Pharmacology, Faculty of Health and Medical Sciences, University of Copenhagen, Universitetsparken 2, DK-2100 Copenhagen, Denmark

Abstract

The zinc-activated channel (ZAC) is a cationic ion channel belonging to the superfamily of Cys-loop receptors, which consists of pentameric ligand-gated ion channels. ZAC is the least understood member of this family so in the present study we sought to characterize the properties of this channel further. We demonstrate that not only zinc (Zn^{2+}) but also copper (Cu^{2+}) and protons (H^+) are agonists of ZAC, displaying potencies and efficacies in the rank orders of $H^+ > Cu^{2+} > Zn^{2+}$ and $H^+ > Zn^{2+} > Cu^{2+}$, respectively. The responses elicited by Zn^{2+}, Cu^{2+} and H^+ through ZAC are all characterized by low degrees of desensitization. In contrast, currents evoked by high concentrations of the three agonists comprise distinctly different activation and decay components, with transitions to and from an open state being significantly faster for H^+ than for the two metal ions. The permeabilities of ZAC for Na^+ and K^+ relative to Cs^+ are indistinguishable, whereas replacing all of extracellular Na^+ and K^+ with the divalent cations Ca^{2+} or Mg^{2+} results in complete elimination of Zn^{2+}-activated currents at both negative and positive holding potentials. This indicates that ZAC is non-selectively permeable to monovalent cations, whereas Ca^{2+} and Mg^{2+} inhibit the channel. In conclusion, this is the first report of a Cys-loop receptor being gated by Zn^{2+}, Cu^{2+} and H^+. ZAC could be an important mediator of some of the wide range of physiological functions regulated by or involving Zn^{2+}, Cu^{2+} and H^+.

Keywords

Zinc; Copper; Protons; Cys-loop ligand-gated ion channels; Calcium block

*Corresponding author at: Department of Neuroscience, Tufts University School of Medicine, 136 Harrison Ave, Boston, MA 02111, USA.

Authorship contributions

Participated in research design: Trattnig, Gasiorek, Deeb, Ortiz, Moss, Jensen, and Davies.
Conducted experiments: Trattnig, Gasiorek, and Davies.
Performed data analysis: Trattnig, Gasiorek, Deeb, and Davies.
Wrote or contributed to the writing of the manuscript: Trattnig, Gasiorek, Deeb, Ortiz, Moss, Jensen, and Davies.

The authors declare no competing financial interests.

1. Introduction

The zinc-activated channel (ZAC) is a ligand-gated ion channel (LGIC) belonging to the Cys-loop receptor superfamily which also includes the nicotinic acetylcholine (nACh), 5-hydroxytryptamine type-3 (5-HT_3), γ-aminobutyric acid type A ($GABA_A$) and glycine receptors [1]. These classical members of this superfamily play important roles in physiology and pathology and thus constitute interesting drug targets in a wide range of disorders [2–5]. ZAC is the least understood member of this family, partly because the gene encoding for ZAC is a pseudogene in mouse and rat genomes, which has complicated explorations into the physiological function of the receptor [1,6].

ZAC displays very little amino acid sequence similarity with other members in the superfamily, and thus it is classified within its own subgroup, the closest matches to ZAC being the human 5-HT3A, 5-HT3B and nACh α7 subunits that exhibit approximately 15% amino acid sequence identity to ZAC [1,6]. Expression studies have detected ZAC mRNA in human fetal whole brain, spinal cord, pancreas, placenta, prostate, thyroid, trachea and stomach [1,6]. Furthermore, the presence of ZAC mRNA has been demonstrated by RT-PCR in adult human hippocampus, striatum, amygdala and thalamus [6]. The presence of ZAC has also been demonstrated in human hippocampal CA3 pyramidal cells and in the polymorphic layer of the dentate gyrus by immunolocalization techniques [6].

Transition metals are known to be essential for proper functioning of various proteins critical for cellular viability and for numerous cellular processes, and thus the intracellular and extracellular concentrations of metals are tightly regulated by metal binding proteins and metal specific transporters [7,8]. Additionally, metal ions can influence the activity of cells by modulating various ion channels, no more so than within the CNS where zinc (Zn^{2+}) and other metals are recognized as neuromodulators of N-methyl-D-aspartate, $GABA_A$, nACh, 5-HT_3 and glycine receptors [9]. Zn^{2+} is essential for normal prenatal and postnatal development and is especially important for fetal brain function [10]. Levels of Zn^{2+} and other metals also appear to be important in neurodegenerative disorders such as Alzheimer's disease as well as other neurological disorders that result in neuronal loss, including epilepsy and ischemia [11–14]. Within the periphery, metals play important roles in the proper functioning of gastrointestinal, immune and reproductive systems [10]. The pancreas and prostate accumulate and release abundant Zn^{2+} and impairment of Zn^{2+} signaling is associated with diabetes, infertility and cancer [15]. Hence, given the overlapping location of ZAC and the systems affected by imbalances in metal signaling, the receptor may govern important functions for human health.

In our previous study of ZAC, this channel was shown to spontaneously open (open in the absence of agonist) when expressed in human embryonic kidney 293 (HEK293) cells, and application of Zn^{2+} was found to evoke a reversible inward current [1]. However, the small amplitudes of Zn^{2+}-activated currents through ZAC in HEK293 cells hampered the investigation of the properties of the channel. In the present study, we have explored further the functional properties of ZAC expressed in COS-7 cells, another mammalian cell line often employed to study recombinant proteins. We report the discovery of two additional

agonists for ZAC (Cu^{2+} and H^+) and present new findings about the biophysical properties of the receptor.

2. Materials and methods

2.1. Cell culture and transfections

COS-7 cells (ATCC CRL-1651) and HEK293 cells (ATCC CRL-1573) were cultured in Dulbecco's Modified Eagle's Medium supplemented with 10% calf serum, 100 i.u./ml penicillin and 100 μg/ml streptomycin at 37 °C in a humidified 5% CO_2, 95% air atmosphere. Cells were electroporated (110 V, 20 ms Biorad Gene Pulser Xcell, Hercules, CA) with cDNA encoding for human ZAC along with GFP cDNAs (in pCDM8). Both cDNAs encoding a myctagged and the un-tagged ZAC were used, and since no differences in agonist-evoked current characteristics were observed between cells electroporated with the two constructs, the data were pooled. Cells were used 24–72 h after electroporation.

2.2. Patch-clamp electrophysiology

The whole-cell configuration of the patch-clamp technique was used to record currents from voltage-clamped COS-7 cells. For agonist concentration–response relationship experiments, cells were superfused, at a rate of 2 ml/min, with an extracellular solution containing (in mM): 140 NaCl, 5 KCl, 1.2 $MgCl_2$, 2.5 $CaCl_2$, 10 3-(N-morpholino)propanesulfonic acid (MOPS), 11 glucose and adjusted to pH 7.4 with NaOH. MOPS was used in this study as it is a Good's zwitterionic buffer that does not form complexes with the metals, unlike the typical HEPES buffer [16]. Borosilicate glass patch pipettes (resistance 2–5 MΩ) contained (in mM): 140 KCl, 2 $MgCl_2$, 0.1 $CaCl_2$, 1.1 EGTA, 10 HEPES, and adjusted to pH 7.4 with KOH.

In the experiments on H^+-activated currents, acidic solutions that were rapidly applied to ZAC-expressing cells consisted of extracellular solutions adjusted to a pH of 7.0 with HCl. Solutions with a pH range from 4.5 to 6.5 were made up fresh on the day of experiments from addition of HCl to a solution containing (in mM): 110 NaCl, 5 KCl, 1.2 $MgCl_2$, 2.5 $CaCl_2$, 10 Trisodium citrate dihydrate, 11 glucose. In the ion substitution experiments, Zn^{2+}-activated currents were recorded in extracellular solution (E1) where KCl was replaced with additional NaCl and both $MgCl_2$ and $CaCl_2$ were reduced to lower their influence upon zinc-mediated current amplitude. E1 consisted of (in mM): 145 NaCl, 0.1 $MgCl_2$, 0.1 $CaCl_2$, 10 MOPS, 11 glucose, adjusted to pH 7.4 with measured amounts of NaOH. To determine the permeability of K^+ relative to Cs^+ E1 was exchanged with E2 where all NaCl in E1 was replaced with KCl (pH adjusted with KOH). Extracellular solution E1 was exchanged with solution E3 or E4 to determine the permeability of Ca^{2+} and Mg^{2+} relative to Cs^+ respectively. These solutions consisted of (in mM): 100 $CaCl_2$ ($MgCl_2$ for E4), 5 histidine, 10 glucose (pH 7.4). Intracellular recording solution (I1) contained (in mM) 140 CsCl, 2 $MgCl_2$, 0.1 $CaCl_2$, 1.1 EGTA, 10 HEPES, adjusted to pH 7.4 with CsOH. The free intracellular calcium concentration was estimated to be 10 nM [17].

Experiments examining the inhibitory properties of Ca^{2+} and Mg^{2+} at ZAC were conducted with recording solutions I1 and E1 (as detailed above). The concentration of extracellular

Ca^{2+} was then raised from 0.1 mM to between 1 and 75 mM by the addition of $CaCl_2$. Studies examining the block of ZAC by Mg^{2+} were conducted by raising the $MgCl_2$ concentration to 30 mM. Solutions containing the raised concentrations of Ca^{2+} and Mg^{2+} in the presence or absence of Zn^{2+} were focally applied to the cell via a SF-77B fast-step perfusion system (Warner Inst., Hamden, CT).

Agonists were applied to GFP-positive cells via the fast-step perfusion system. All experiments were carried out at 32–33 °C using a recording chamber and in-line perfusion heaters (Warner Inst.). Typically, liquid junction potentials were nulled with an open electrode in the recording chamber prior to experiments. For the ion substitution studies, liquid junction potentials were measured with an open-tipped electrode and corrected post hoc. Cells were voltage-clamped at −60 mV unless otherwise noted.

2.3. Data acquisition and analysis

Currents were recorded with an Axopatch 200B amplifier (Molecular Devices, Sunnyvale, CA), filtered at 2 kHz and digitized at 20 kHz with a Digidata 1320A (Molecular Devices) and analyzed using either Clampfit (pClamp, Molecular Devices) or Graphpad Prism v.4 software (Graphpad Software, Inc., San Diego, CA). All data are expressed as the arithmetic mean ± S.E.M., and, unless stated otherwise, statistical comparisons were made using the student *t*-test with statistical significance set at $p < 0.05$.

ZAC-mediated currents exhibit an increase in current amplitude over the course of the experiment [1]. To compensate for this run-up phenomenon during concentration–response experiments 1mMZn^{2+} was applied before the subsequent agonist application. The amplitudes of the agonist-evoked currents were normalized to the current elicited by the prior application of 1 mM Zn^{2+}. Concentration– response relationships were fitted by nonlinear regression to a sigmoidal dose–response with variable slope equation (Graphpad).

Time constants for activation and decay of ZAC-activated currents evoked by maximal concentrations of Zn^{2+} (1 mM), Cu^{2+} (30 μM), or H^+ (10 μM, pH 5) were determined by fitting exponential functions to the corresponding component of the current wave form using the Levenberg–Marquardt algorithm with least squares minimization (Clampfit Ver. 9.2; Molecular Devices). A period of time (approximately 10 min) after the establishment of the whole-cell configuration was allowed before the ZAC-activated currents were used for analysis. This allowed for changes in current waveform that occurred during run-up to stabilize. The activation phase of the macroscopic current (between 10% and 90% of peak current amplitude) was fitted by a single exponential function. The rate of current decay upon removal of Zn^{2+}, Cu^{2+} or H^+ was determined by fitting traces to exponential equations from the start of current decay to a point at which 90% of the current had decayed toward baseline. Decay components were best fit to two or more exponentials. To allow for comparisons, weighted time constants were calculated. Time constant values $\tau_{activation}$ and τ_{decay} for different agonists were compared for significant differences using a one-way ANOVA analysis and Bonferroni posttest in Graphpad InStat3 (San Diego, CA).

The reversal potential for ZAC-activated currents (E_{ZAC}) was determined by ramping the membrane potential from −60 mV to 40 mV (within 1 s) in the absence of agonist and

during the plateau phase of the agonist-evoked current. Currents generated during a ramp in the absence of agonist were subtracted from ramp currents in the presence of agonist. Permeability ratios for monovalent cations relative to Cs^+ (P_X/P_{Cs}) were calculated using the Goldman–Hodgkin–Katz voltage equation:

$$E_{Zn} = \frac{RT}{F} \ln \frac{(P_X/P_{Cs})[X^+]_o}{[Cs^+]_i}$$

where E_{Zn} is the equilibrium potential of Zn^{2+}-activated current RT/F is 26.3 mV at 32 °C, $[Cs^+]_i$ and $[X^+]_o$ are the calculated activities of internal Cs^+ and external monovalent ions, respectively. Individual current–voltage relationships obtained during the voltage-ramp were plotted, and a linear fit to points either side of current reversal was used to calculate the equilibrium potential. Equilibrium potentials were averaged. The ionic activities were calculated by multiplying the ionic concentration by the ion activity coefficient (γ_{ion}). The γ_{ion} values were estimated to be: γ_K 0.75, γ_{Cs} 0.72, and γ_{Na} 0.76 [17].

2.4. Drugs and reagents

Tissue culture reagents were purchased from Gibco (Life Technologies Corp., Grand Island, NY, USA), amiloride was purchased from Tocris (Minneapolis, MN), and all other reagents were from Sigma–Aldrich (St. Louis, MO). Metal ion solutions readily hydrolyze to form metal-hydroxy and metal-oxy polymers. These polymers may not always form a visible precipitate but can be biologically inert by preventing the interaction of metals with proteins or cause the metal to bind nonspecifically to a protein through electrostatic interactions rather than to high affinity binding sites [18]. To prevent this hydrolysis, metal stock solutions were made with ligands at a metal:ligand molar ratio of 1:6. The metal:ligand combinations used were; Zn(II)–histidine, Cu(II)–glycine, and Fe(II)–citrate [19]. When tested alone, the ligands histidine, glycine and citrate did not activate ZAC (data not shown).

3. Results

3.1. Expression of ZAC in COS-7 cells

In our previous study, transient expression of ZAC in HEK293 cells was found to yield small Zn^{2+}-activated currents [1]. We therefore examined another cell line to see if it was more suited for ZAC studies. We transiently expressed ZAC in the African Green monkey kidney COS-7 cell line, and performed the experiments at 32–34 °C. Expressing ZAC in COS-7 cells gave consistently larger Zn^{2+}-activated currents than those evoked through the receptor in HEK293 cells (50–200 pA at the start of the experiment in HEK293 cells compared to 200 pA–3 nA at the start of the experiment in COS-7 cells using similar experimental conditions).

Initially, the properties of Zn^{2+} on ZAC transiently expressed in COS-7 cells were investigated. The amplitudes of Zn^{2+}-activated currents, recorded from ZAC-expressing COS-7 cells voltage-clamped at −60 mV, increased with increasing concentrations of Zn^{2+} (Fig. 1A). At a Zn^{2+} concentration of 3 mM, the activated currents displayed marked desensitization in the continued presence of the agonist. Fitting the concentration–response

data with a sigmoidal equation provided an EC_{50} value of 180 μM and a Hill coefficient of 2.2 ± 0.2 for Zn^{2+} (n = 3–5 cells, Table 1). Thus, the properties of ZAC expressed in COS-7 cells were very similar to those previously determined in HEK293 cells [1].

3.2. Ionic permeabilities of ZAC

The ZAC protein shares some identity within the cationic subdivision of Cys-loop receptors, the 5-HT_3 and nACh receptors [1]. Comparing the reversal potentials associated with changes in the ionic composition of intracellular and extracellular solutions we have previously shown that ZAC is impermeable to anions [1]. In the present study, we examined which cations permeate the ZAC ion channel using extracellular solutions of different ionic compositions to compare the permeabilities of the physiological relevant cations Na^+, K^+, Ca^{2+}, and Mg^{2+} relative to intracellular Cs^+.

The relative permeability ratios, P_X/P_{Cs}, of ZAC channels were calculated by determining the reversal potentials of 1 mM Zn^{2+}-activated currents (E_{Zn}) from voltage ramps (Fig. 2A). Reversal potentials were determined in extracellular solutions with differing ionic compositions (see Section 2). Using NaCl-based extracellular solution and CsCl-based intracellular solution E_{Zn} was −11 ± 2 mV corresponding to a P_{Na}/P_{Cs} of 0.65 ± 0.05 (n = 8). When extracellular NaCl was completely replaced with KCl, E_{Zn} was −8 ± 1 mV corresponding to a P_K/P_{Cs} of 0.72 ± 0.04 (n = 7). Hence, there was no significant difference in the permeability of Na^+ and K^+ (t-test, p = 0.29).

When all extracellular monovalent cations were replaced with either Ca^{2+} or Mg^{2+} no detectable Zn^{2+}-activated inward current was observed. Subtracting the current during application of voltage ramps in the absence of Zn^{2+} to that in the presence of Zn^{2+} resulted in no current, suggesting that neither inward nor outward current flowed due to inhibition of ZAC by Ca^{2+} and Mg^{2+} (Fig. 2C).

3.3. Channel inhibition by Ca^{2+} and Mg^{2+}

We further examined the apparent inhibition of ZAC by Ca^{2+} and Mg^{2+} observed in the experiments presented in Fig. 2B and C, and found that ZAC-activated currents evoked by 1mM Zn^{2+} were inhibited by extracellular Ca^{2+} and Mg^{2+}. With a fixed concentration of extracellular Mg^{2+} (0.1 mM), increasing the concentration of Ca^{2+} from 0.1 mM to 75 mM caused a concentration-dependent reversible inhibition of the Zn^{2+}-activated currents (Fig. 3A and B). The IC_{50} value for Ca^{2+} to inhibit ZAC was 9.3 mM (pIC_{50} = 2.03 ± 0.07, n = 6–9 cells). In order to examine any potential voltage-dependence to the inhibition by Ca^{2+}, 1mM Zn^{2+}-activated currents were measured at −60 mV and 60 mV. Inhibition exerted by 30 mM Ca^{2+} was the same at both holding potentials, 47 ± 4% of control (n = 9) at −60 mV and 50 ± 10% of control (n = 4) at 60mV (p = 0.83, Fig. 3C). The inhibition of ZAC by Mg^{2+} was examined by co-applying Zn^{2+}(1 mM) with Mg^{2+} (30 mM) with a fixed concentration of extracellular Ca^{2+} (0.1 mM). In the presence of Mg^{2+} (30 mM), the Zn^{2+}-activated currents were inhibited by 63 ± 0.6% of control (n = 3, Fig. 3A and B). At 30 mM, Ca^{2+} and Mg^{2+} produced a similar degree of inhibition (p = 0.067).

The ability of Ca^{2+} and Mg^{2+} to inhibit the current conductance through ZAC could be caused by inhibiting Zn^{2+} binding via a surface charge screening effect on the surface of

ZAC [20]. We examined the inhibition by Ca^{2+} of the spontaneous ZAC-mediated current in the absence of agonist. At a holding potential of −60 mV, application of Ca^{2+} (30 mM) evoked a reversible outward current, which was caused by the inhibition of the spontaneous inward current, that was 22 ± 3.5% of a preceding 1 mM Zn^{2+}-activated current (n = 3, Fig. 3D). Thus, Ca^{2+} inhibits the channel itself rather than inhibiting the binding of Zn^{2+} to the channel.

3.4. Copper is an agonist of ZAC

Next we examined the putative ZAC activating properties of several additional transition metals. Rapid applications of iron (Fe^{2+}), cobalt (Co^{2+}), nickel (Ni^{2+}), cadmium (Cd^{2+}), and aluminum (Al^{3+}), all applied at a concentration of 1 mM, did not produce any ZAC-mediated currents (Fig. 4). In contrast, 1 mM Cu^{2+} evoked a large inward current in cells transfected with ZAC (Fig. 5), but not in untransfected COS-7 cells (data not shown). Cu^{2+} evoked currents in a concentration dependent manner up to 30 μM, whereas currents evoked by Cu^{2+} concentrations greater than 30 μM were characterized by reduced amplitudes (Fig. 5A). Thus, the resulting concentration–response relationship of Cu^{2+} was biphasic. The activating component exhibited an EC_{50} value of 4.0 μM, an estimated Hill coefficient of 3.3, and a maximal response of 52 ± 3% of the response evoked by 1 mM Zn^{2+} (n = 3–14 cells, Fig. 5B, Table 1).

3.5. H^+ is an agonist of ZAC

The expression of ZAC in the stomach [1] prompted us to test the putative effects of protons on ZAC signaling. Application of low pH solutions to COS-7 cells expressing ZAC evoked a reversible inward current at −60 mV (Fig. 6A). ZAC was activated by H^+ in a concentration-dependent manner, displaying a pH_{50} value of 5.6 ± 0.1, a Hill coefficient of 3.7 ± 2.5, and a maximal response of 142 ± 10% of the response evoked by 1 mM Zn^{2+} (n = 4–6 cells, Fig. 6B, Table 1). This pH_{50} corresponded to a H^+ EC_{50} of 2.3 μM. Analogously to the Zn^{2+}- and Cu^{2+}-activated currents, an increase in current desensitization was observed in the presence of higher H^+ concentrations (Fig. 6A).

3.6. Activation and decay kinetics of Zn^{2+}, Cu^{2+} and H^+ activated currents through ZAC

During the characterization of the concentration–response relationships of Zn^{2+}, Cu^{2+} and H^+, it became apparent that high concentrations of the three agonists gave rise to currents characterized by different activation and decay components. Comparison of τ values obtained for the activation and decay phases of ZAC-mediated currents revealed significant differences for the three agonists at maximal concentrations (Fig. 7A and B). Currents activated by Zn^{2+} (1 mM) peaked at later time-points, resulting in higher $\tau_{activation}$ values (τ = 585 ± 70 ms, n = 3) compared to 30 μM Cu^{2+}-activated currents (τ = 367 ± 85 ms, n = 3, $p < 0.05$, unpaired t-test), and 10 μM H^+ (pH 5)-activated currents (τ = 234 ± 52 ms, n = 3, $p < 0.01$, unpaired t-test). Decay of peak current amplitude to baseline after H^+ exposure (τ = 198 ± 33 ms, n = 3) was also markedly faster compared to currents activated by Cu^{2+} (τ = 706 ± 54 ms, n = 3, $p < 0.01$, unpaired t-test) or Zn^{2+} (τ = 697 ± 89 ms, n = 3, $p < 0.01$, unpaired t-test).

The proton-mediated currents recorded in COS-7 cells expressing ZAC are similar to those mediated by the prokaryotic proton-gated Cys-loop receptor ortholog GLIC in that they show little desensitization [21]. This is in marked contrast to the desensitization observed with acid-sensing ion channels (ASICs). HEK293 cells endogenously express ASICs that exhibit large amplitude, fast activating currents that desensitize in the continued presence of protons. Additionally, ASIC-mediated currents are blocked in the presence of extracellular amiloride [22]. When ZAC is expressed in HEK293 cells, a typical ZAC-mediated current is observed with the application of zinc. However, an application of pH 5.5 sometimes evoked a larger, faster activating, desensitizing current that is more typical of a ASIC-mediated current (Fig. 8A). When H^+ was co-applied with 100 μMamiloride, only ZAC-like, slow activating non-desensitizing currents were observed (Fig. 8B).

4. Discussion

The present study elaborates on our original discovery of the human Cys-loop receptor ZAC [1]. We demonstrate that Cu^{2+} and H^+ also are agonists of ZAC, which consequently should be considered a Zn^{2+}, Cu^{2+}- and pH-sensing receptor.

Consistent with our previous study of ZAC expressed in HEK293 cells [1], the currents elicited by Zn^{2+}, Cu^{2+} and H^+ through the receptor expressed in COS-7 cells were all characterized by a lack of macroscopic desensitization at most concentrations. Only at high agonist concentrations did macroscopic desensitization become apparent, reducing peak current amplitude and resulting in a bi-phasic agonist concentration–response relationship, which is most notable with Cu^{2+} but also observed for Zn^{2+} and H^+ (Figs. 1, 5 and 6). Cu^{2+} and H^+ displayed 40- and 72-fold higher potencies than Zn^{2+}, respectively. Furthermore, H^+ exhibited ~1.5-fold higher efficacy compared to Zn^{2+}, whereas the maximal response elicited by Cu^{2+} was only half of that evoked by Zn^{2+} (Figs. 1, 5 and 6).

The responses elicited by the three agonists were characterized by distinct activation and decay components. When maximal concentrations of the agonists were used, Zn^{2+}-evoked currents activated slower than both Cu^{2+}- and H^+-evoked currents, whereas the decay from peak amplitudes of H^+-evoked currents was markedly faster than the decay of Zn^{2+}- and Cu^{2+}-evoked currents. At these agonist concentrations, the decay phase would have components of transitions out of the desensitized state and deactivation. The differences in channel characteristics observed for the agonists would suggest that ZAC transitions to and from an open state faster when activated by H^+ than the metal ions. However, in-depth kinetic studies using ultra-rapid agonist application systems followed by kinetic modeling [23] will be needed to further elucidate the gating kinetics of the respective agonists.

ZAC is a cation-selective channel [1], and in the present study the rank order of permeability to monovalent cations was found to be $Cs^+ > K^+ = Na^+$. This characteristic is very similar to the monovalent cation permeability of 5-HT_3A receptors [17]. In contrast to the Ca^{2+} and Mg^{2+} permeability of 5-HT_3A and nACh α7 receptors [24,25], our data indicate that ZAC is not only impermeable to both divalent cations, but that the ions also inhibit the channel. In previous studies several residues in the outer extracellular (20′) and cytoplasmic rings (−4′) of transmembrane domain 2 (TM2) in 5-HT_3A and nACh α7 receptors as well as the Asp^{127}

in the extracellular vestibule of 5-HT_3A have been identified as determinants of the divalent cation permeability of these receptors [24,26–28]. An alignment of the amino acid sequences of ZAC, 5-HT3A and α7 subunits predicts the corresponding residues in ZAC to be Gln (TM2 20′: Asp^{293} in 5-HT_3A, Glu^{281} in nAChα7), Arg (Asn^{269} in TM2 −4′ ring in 5-HT_3A, Asp^{257} in nAChα7) and Trp (Asp^{127} in 5-HT_3A, Asp^{119} in nAChα7), and we propose that these substantial differences in the physicochemical properties of the residues at these positions of ZAC are likely to contribute to the impermeability of Ca^{2+} and Mg^{2+}. If ZAC was simply impermeable to Ca^{2+} and Mg^{2+}, then one would expect to observe an outward Cs^{+} current at positive potentials. The absence of this current when extracellular Na^{+} were replaced with either Ca^{2+} or Mg^{2+} suggests that the divalent cations inhibit ZAC.

The voltage-independent inhibition of Zn^{2+}-activated currents caused by Ca^{2+} and Mg^{2+} could be due to a change in the affinity of Zn^{2+} by altering surface potential through the charge screening of residues [20]. However, ZAC is a spontaneously active ion channel [1] that can open in the absence of an agonist. Application of Ca^{2+} alone inhibited ZAC-mediated spontaneous current, similar to the effect seen when the antagonist, tubocurarine, is applied in the absence of Zn^{2+} [1]. The ability of Ca^{2+} to inhibit the channel in the absence of agonist suggests that the divalent cations are inhibiting ZAC not by preventing Zn^{2+} (or other agonists) binding but by physically inhibiting the ion channel.

The sizes and the physicochemical properties of the three agonists identified for ZAC differs substantially from the endogenous agonists of other mammalian Cys-loop LGICs (ACh, serotonin, GABA and glycine). The location and molecular composition of the consensus orthosteric site in these ‘classical’ Cys-loop receptors are highly conserved. Typically, transmitter binding to these receptors is mediated by an ‘aromatic box’ formed by five aromatic residues, where the quaternary ammonium or protonated amino group of the ligand forms a cation-π interaction with an aromatic residue [29]. Although these aromatic residues are not completely conserved throughout the Cys-loop receptor family a certain degree of consensus exists. Thus, it is striking that none of these aromatic residues are conserved in ZAC. In view of this and the markedly different chemical nature of Zn^{2+}, Cu^{2+} and H^{+} compared to the organic transmitters, it seems unlikely that an analogous site exists in ZAC. In ongoing studies in our labs we are investigating whether the underlying mechanism for proton-gating of ZAC could be similar to that proposed for the prokaryotic proton-gated Cys-loop receptor ortholog GLIC [30,31].

As neighbors in the periodic table of elements, the physicochemical properties of Zn^{2+} and Cu^{2+} are similar, furthermore their biological functions also overlap. Like Zn^{2+}, Cu^{2+} constitutes a structural component of many proteins, functions as a key cofactor for the catalytic activity of numerous enzymes, and modulates the activity of several ion channels [9,32,33]. Extracellular Cu^{2+} concentration is regulated by the cellular uptake mediated by the transporter CTR1 and the Cu^{2+} export from cells by the ATPases ATP7A and ATP7B [32–34]. To our knowledge, ZAC is the first receptor ion channel shown to be directly activated by Cu^{2+}.

The discoveries of the proton-gated Cys-loop receptor orthologs GLIC and PBO-5/6 in *Gloeobacter violaceus* and *Caenorhabditis elegans*, respectively, suggest a conserved role for

these receptors in pH-sensing [21,35]. The proton-evoked ZAC signaling in this study takes place between pH 5 and 6. This would suggest that ZAC could be physiologically relevant in tissues characterized by slightly acidic conditions, such as the stomach or in pathological acidic conditions.

Physiological concentrations of Zn^{2+}, Cu^{2+} and H^+ are notoriously difficult to measure because free ions rapidly associate with various proteins, and it is unclear if bound Zn^{2+}, Cu^{2+} and H^+ are available to modulate ion channels. Prostate fluid has some of the highest Zn^{2+} content outside the brain; 9 mM [36]. In the CNS, concentrations of Zn^{2+}, Cu^{2+} and H^+ are in the low micromolar range but concentrations from vesicle release into the synaptic cleft are in the 10–200 μM range and even higher in neurodegenerative diseases [9,33,37,38]. However, alternative mechanisms to vesicular release of zinc are possible [39,40]. The pH of extracellular solutions are tightly controlled but synaptic vesicles have high proton concentrations (pH 5.7) such that elevated vesicle release during high neuronal activity could lower the pH in the synaptic cleft [41].

In light of the discovery of Cu^{2+} and H^+ as ZAC agonists the hypotheses about putative physiological functions of this receptor clearly have to be revised. The fact that both Zn^{2+} and Cu^{2+} and protons activate ZAC in physiologically relevant concentration ranges highlights the potential importance of the receptor in various native tissues. As a promiscuous cation channel activated not only by Zn^{2+} but also by Cu^{2+} and H^+, ZAC could be envisioned to mediate effects by all three agonists in regions known to contain these agonists in considerable concentrations such as different regions of the CNS, stomach, prostate, and pancreas.

This present study has demonstrated that ZAC forms an ion channel gated by Zn^{2+}, Cu^{2+}, and H^+ and is non-selectively permeable to monovalent cations. The role of ZAC in Zn^{2+}, Cu^{2+}, and H^+ signaling requires further investigation and could be part of an unexplored signaling cascade that may provide new therapeutic strategies for a number of pathological conditions.

Acknowledgments

This work was supported by grants from the National Institutes of Health (NIH)-National Institute of Alcoholism and Alcohol Abuse grant AA017938 (P.A.D.), NIH-National Institute of Mental Health grant MH097446 (P.A.D. and S.J.M.), NIH-National Institute of Neurological Disorders and Stroke grant NS036296, NS047478, NS048045 and NS054900 (S.J.M.), NS061764 training fellowship (E.J.C.O.), the Lundbeck Foundation (S.M.T. and A.A.J.) and the Novo Nordisk Foundation (A.A.J.).

We would like to thank Drs. Tim Hales and Daniel Baptista-Hon for their invaluable advice and comments.

Abbreviations

ZAC	zinc-activated channel
LGIC	ligand-gated ion channel
nACh	nicotinic acetylcholine
5-HT	5-hydroxytryptamine

GFP	green fluorescent protein
MOPS	10 3-(N-morpholino)propanesulfonic acid
CTR1	high affinity copper uptake protein 1
GLIC	*Gloeobacter violaceus* pentameric ligand-gated ion channel
ATP7A, ATPase	Cu^{2+} transporting, alpha polypeptide
ATP7B, ATPase	Cu^{2+} transporting, beta polypeptide

References

1. Davies PA, Wang W, Hales TG, Kirkness EF. A novel class of ligand-gated ion channel is activated by Zn^{2+} . J. Biol. Chem. 2003; 278:712–717. [PubMed: 12381728]
2. Taly A, Corringer PJ, Guedin D, Lestage P, Changeux JP. Nicotinic receptors: allosteric transitions and therapeutic targets in the nervous system. Nat. Rev. Drug Discov. 2009; 8:733–750. [PubMed: 19721446]
3. Barnes NM, Hales TG, Lummis SC, Peters JA. The 5-HT3 receptor – the relationship between structure and function. Neuropharmacology. 2009; 56:273–284. [PubMed: 18761359]
4. Olsen RW, Sieghart W. International Union of Pharmacology. LXX. Subtypes of gamma-aminobutyric acid (A) receptors: classification on the basis of subunit composition, pharmacology, and function. Update. Pharmacol. Rev. 2008; 60:243–260. [PubMed: 18790874]
5. Lynch JW. Native glycine receptor subtypes and their physiological roles. Neuropharmacology. 2009; 56:303–309. [PubMed: 18721822]
6. Houtani T, Munemoto Y, Kase M, Sakuma S, Tsutsumi T, Sugimoto T. Cloning and expression of ligand-gated ion-channel receptor L2 in central nervous system. Biochem. Biophys. Res. Commun. 2005; 335:277–285. [PubMed: 16083862]
7. Chasapis CT, Loutsidou AC, Spiliopoulou CA, Stefanidou ME. Zinc and human health: an update. Arch. Toxicol. 2011
8. Fukada T, Yamasaki S, Nishida K, Murakami M, Hirano T. Zinc homeostasis and signaling in health and diseases: zinc signaling. J. Biol. Inorg. Chem. 2011; 16:1123–1134. [PubMed: 21660546]
9. Mathie A, Sutton GL, Clarke CE, Veale EL. Zinc and copper: pharmacological probes and endogenous modulators of neuronal excitability. Pharmacol. Ther. 2006; 111:567–583. [PubMed: 16410023]
10. Hambidge M. Human zinc deficiency. J. Nutr. 2000; 130:1344S–1349S. [PubMed: 10801941]
11. Bush AI. Copper, zinc, and the metallobiology of Alzheimer disease. Alzheimer Dis. Assoc. Disord. 2003; 17:147–150. [PubMed: 14512827]
12. Frederickson CJ, Koh JY, Bush AI. The neurobiology of zinc in health and disease. Nat. Rev. Neurosci. 2005; 6:449–462. [PubMed: 15891778]
13. Weiss JH, Sensi SL, Koh JY. Zn(2+): a novel ionic mediator of neural injury in brain disease. Trends Pharmacol. Sci. 2000; 21:395–401. [PubMed: 11050320]
14. Shuttleworth CW, Weiss JH. Zinc: new clues to diverse roles in brain ischemia. Trends Pharmacol. Sci. 2011; 32:480–486. [PubMed: 21621864]
15. Kelleher SL, McCormick NH, Velasquez V, Lopez V. Zinc in specialized secretory tissues: roles in the pancreas, prostate, and mammary gland. Adv. Nutr. 2011; 2:101–111. [PubMed: 22332039]
16. Aslamkhan AG, Aslamkhan A, Ahearn GA. Preparation of metal ion buffers for biological experimentation: a methods approach with emphasis on iron and zinc. J. Exp. Zool. 2002; 292:507–522. [PubMed: 12115934]
17. Brown AM, Hope AG, Lambert JJ, Peters JA. Ion permeation and conduction in a human recombinant 5-HT3 receptor subunit (h5-HT3A). J. Physiol. 1998; 507(Pt 3):653–665. [PubMed: 9508827]

18. Masuoka J, Hegenauer J, Van Dyke BR, Saltman P. Intrinsic stoichiometric equilibrium constants for the binding of zinc(II) and copper(II) to the high affinity site of serum albumin. J. Biol. Chem. 1993; 268:21533–21537. [PubMed: 8408004]
19. Huang F, Bitton G, Kong IC. Determination of the heavy metal binding capacity of aquatic samples using MetPLATE: a preliminary study. Sci. Total Environ. 1999; 234:139–145. [PubMed: 10507154]
20. Green WN, Andersen OS. Surface charges and ion channel function. Annu. Rev. Physiol. 1991; 53:341–359. [PubMed: 1710438]
21. Bocquet N, Prado-de-Carvalho L, Cartaud J, Neyton J, Le-Poupon C, Taly A, et al. A prokaryotic proton-gated ion channel from the nicotinic acetylcholine receptor family. Nature. 2007; 445:116–119. [PubMed: 17167423]
22. Samways DS, Harkins AB, Egan TM. Native and recombinant ASIC1a receptors conduct negligible Ca^{2+} entry. Cell Calcium. 2009; 45:319–325. [PubMed: 19185346]
23. Solt K, Ruesch D, Forman SA, Davies PA, Raines DE. Differential effects of serotonin and dopamine on human 5-HT3A receptor kinetics: interpretation within an allosteric kinetic model. J. Neurosci. 2007; 27:13151–13160. [PubMed: 18045909]
24. Livesey MR, Cooper MA, Lambert JJ, Peters JA. Rings of charge within the extracellular vestibule influence ion permeation of the 5-HT3A receptor. J. Biol. Chem. 2011; 286:16008–16017. [PubMed: 21454663]
25. Wallace TL, Porter RH. Targeting the nicotinic alpha7 acetylcholine receptor to enhance cognition in disease. Biochem. Pharmacol. 2011; 82:891–903. [PubMed: 21741954]
26. Abdel-Aziz H, Windeck T, Ploch M, Verspohl EJ. Mode of action of gingerols and shogaols on 5-HT3 receptors: binding studies, cation uptake by the receptor channel and contraction of isolated guinea-pig ileum. Eur. J. Pharmacol. 2006; 530:136–143. [PubMed: 16364290]
27. Imoto K, Busch C, Sakmann B, Mishina M, Konno T, Nakai J, et al. Rings of negatively charged amino acids determine the acetylcholine receptor channel conductance. Nature. 1988; 335:645–648. [PubMed: 2459620]
28. Livesey MR, Cooper MA, Deeb TZ, Carland JE, Kozuska J, Hales TG, et al. Structural determinants of Ca2+ permeability and conduction in the human 5-hydroxytryptamine type 3A receptor. J. Biol. Chem. 2008; 283:19301–19313. [PubMed: 18474595]
29. Lester HA, Dibas MI, Dahan DS, Leite JF, Dougherty DA. Cys-loop receptors: new twists and turns. Trends Neurosci. 2004; 27:329–336. [PubMed: 15165737]
30. Hilf RJ, Dutzler R. Structure of a potentially open state of a proton-activated pentameric ligand-gated ion channel. Nature. 2009; 457:115–118. [PubMed: 18987630]
31. Wang HL, Cheng X, Sine SM. Intramembrane proton binding site linked to activation of bacterial pentameric ion channel. J. Biol. Chem. 2012; 287:6482–6489. [PubMed: 22084238]
32. Madsen E, Gitlin JD. Copper and iron disorders of the brain. Annu. Rev. Neurosci. 2007; 30:317–337. [PubMed: 17367269]
33. Que EL, Domaille DW, Chang CJ. Metals in neurobiology: probing their chemistry and biology with molecular imaging. Chem. Rev. 2008; 108:1517–1549. [PubMed: 18426241]
34. Lutsenko S, Bhattacharjee A, Hubbard AL. Copper handling machinery of the brain. Metallomics. 2010; 2:596–608. [PubMed: 21072351]
35. Beg AA, Ernstrom GG, Nix P, Davis MW, Jorgensen EM. Protons act as a transmitter for muscle contraction in *C. elegans*. Cell. 2008; 132:149–160. [PubMed: 18191228]
36. Kavanagh JP. Sodium, potassium, calcium, magnesium, zinc, citrate and chloride content of human prostatic and seminal fluid. J. Reprod. Fertil. 1985; 75:35–41. [PubMed: 4032375]
37. Sensi SL, Paoletti P, Koh JY, Aizenman E, Bush AI, Hershfinkel M. The neurophysiology and pathology of brain zinc. J. Neurosci. 2011; 31:16076–16085. [PubMed: 22072659]
38. Hung YH, Bush AI, Cherny RA. Copper in the brain and Alzheimer's disease. J. Biol. Inorg. Chem. 2010; 15:61–76. [PubMed: 19862561]
39. Kay AR, Toth K. Is zinc a neuromodulator? Sci Signal. 2008; 1:re3. [PubMed: 18480018]
40. Kay AR. Evidence for chelatable zinc in the extracellular space of the hippocampus, but little evidence for synaptic release of Zn. J. Neurosci. 2003; 23:6847–6855. [PubMed: 12890779]

41. Miesenbock G, De Angelis DA, Rothman JE. Visualizing secretion and synaptic transmission with pH-sensitive green fluorescent proteins. Nature. 1998; 394:192–195. [PubMed: 9671304]

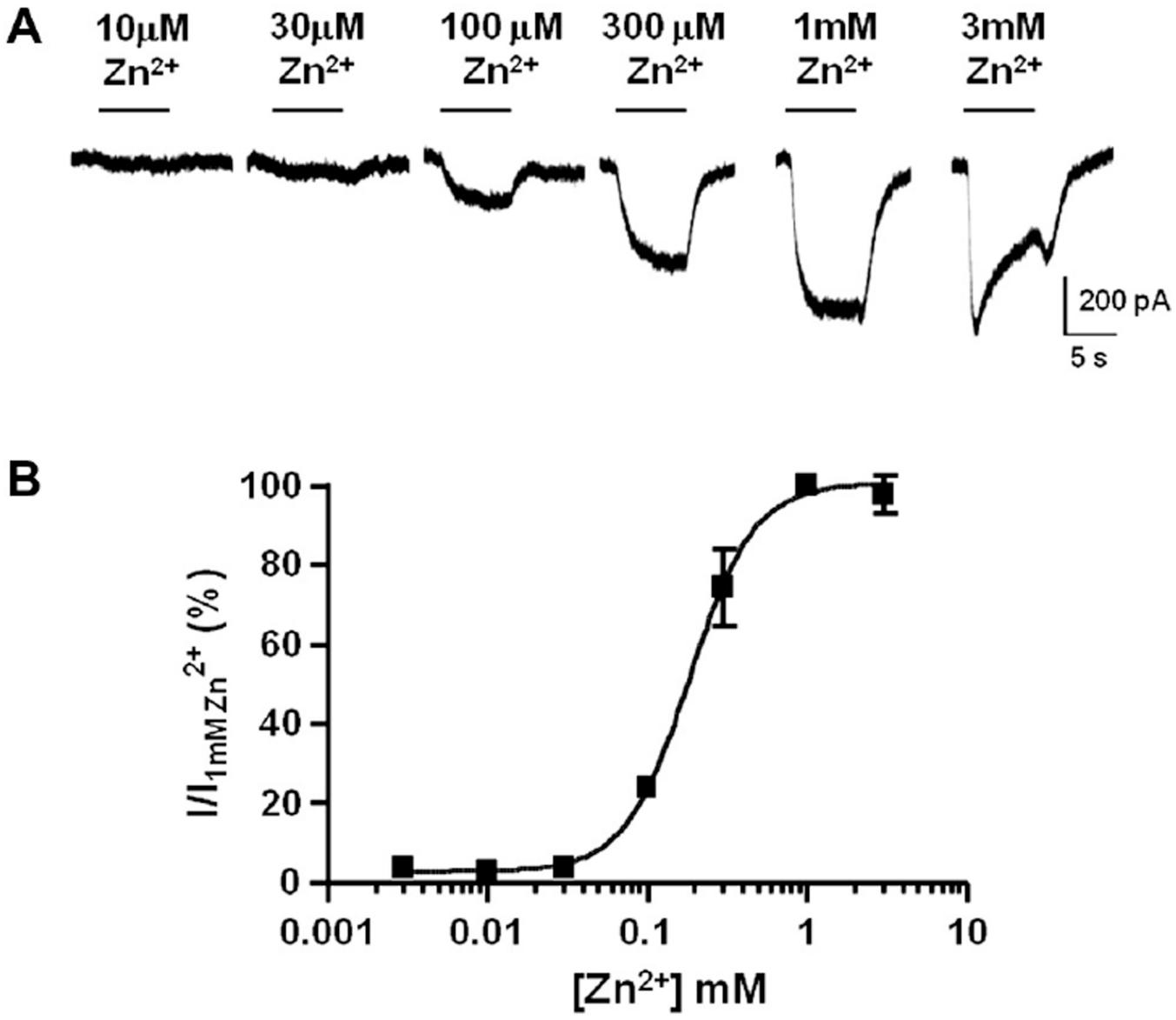

Fig. 1.

Zn^{2+} as a ZAC agonist. (A) Inward currents evoked by rapid applications of Zn^{2+} to ZAC-expressing COS-7 cells. Zn^{2+} was applied (solid bar) for 6 s to cells voltage-clamped at −60 mV Zn^{2+}-mediated currents recorded from COS-7 cells transiently transfected with ZAC. (B) Concentration–response relationship for Zn^{2+} at ZAC-expressing COS-7 cells. Data shown as mean ± S.E.M. generated from 3 to 5 cells.

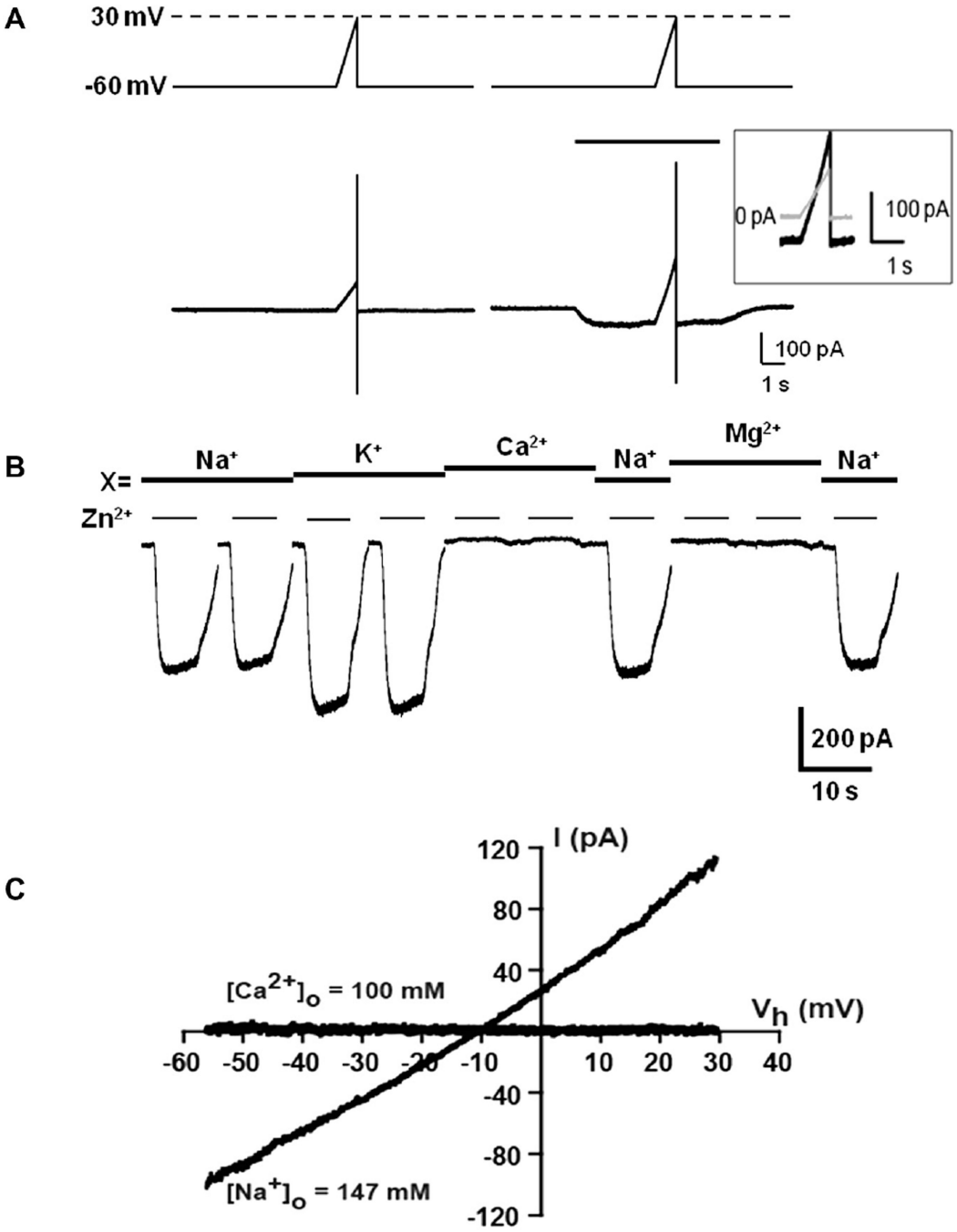

Fig. 2.

Cationic permeability of ZAC. (A). Voltage ramps between −60 mV and 30 mV applied before and during agonist application. Non-specific currents recorded during voltage ramps in the absence of Zn^{2+} were subtracted from currents recorded during voltage ramps applied during the steady state inward current evoked by 1 mMZn^{2+} (solid bar). Insert; overlapping currents evoked by voltage ramps in the absence (gray current) and presence of Zn^{2+} (black current). (B) Representative Zn^{2+}-mediated currents recorded from a ZAC-expressing COS-7 cell in extracellular solutions of varying ionic compositions. Zn^{2+} (1 mM) was

applied 1/60 s (Zn^{2+}-mediated currents are concatenated in the illustration). The major cationic species is indicated above each trace (see Section 2 for details). When all extracellular monovalent cations were replaced with either Ca^{2+} or Mg^{2+} no detectable Zn^{2+}-mediated inward current was observed. (C) Current–voltage relationships from a representative ZAC expressing COS-7 cell obtained from voltage ramps applied during the application of 1 mM Zn^{2+}. The current obtained with a NaCl-based extracellular solution was completely absent when Zn^{2+} was applied with a $CaCl_2$-based solution. The lack of outward current at positive potentials indicates that Ca^{2+} is inhibiting the outward flux of intracellular Cs^{+}.

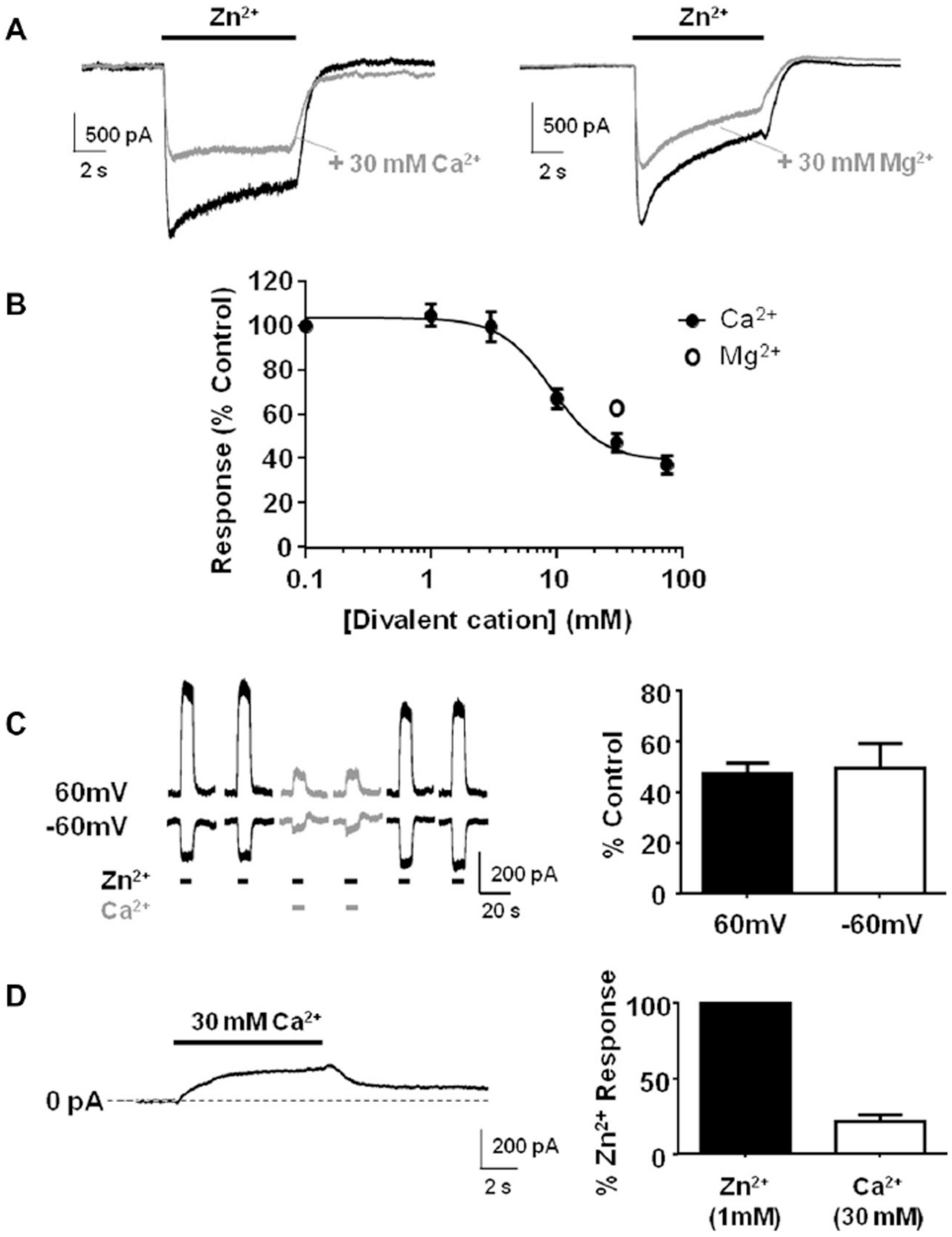

Fig. 3.

Inhibition of ZAC by Ca^{2+} and Mg^{2+}. (A) Overlaid representative Zn^{2+}-evoked current in the absence (black current) or in the presence of 30 mM Ca^{2+} or Mg^{2+} (gray current). (B) Concentration–inhibition relationship of the Ca^{2+} block (closed circles) of ZAC. Block of Zn^{2+}-evoked current by 30 mM Mg^{2+} is also shown (open circle). Data points are mean ± S.E.M., n = 3–9 cells. (C) Voltage-independence of Ca^{2+} block of ZAC. Left: Zn^{2+}-evoked currents at holding potentials of 60 mV and −60 mV in the absence (black currents) and presence of 30 mM Ca^{2+} (gray currents). Right: bar graph showing mean inhibition at 60

mV (n = 4) and −60 mV (n = 9). (D) At a holding potential of −60 mV, application of 30 mM Ca^{2+} evoked a reversible outward current representing the inhibition of spontaneous current. Bar graph showing the mean outward Ca^{2+} (30 mM)-evoked current as a percent of the preceding Zn^{2+} (1 mM)-evoked current (n = 3 cells).

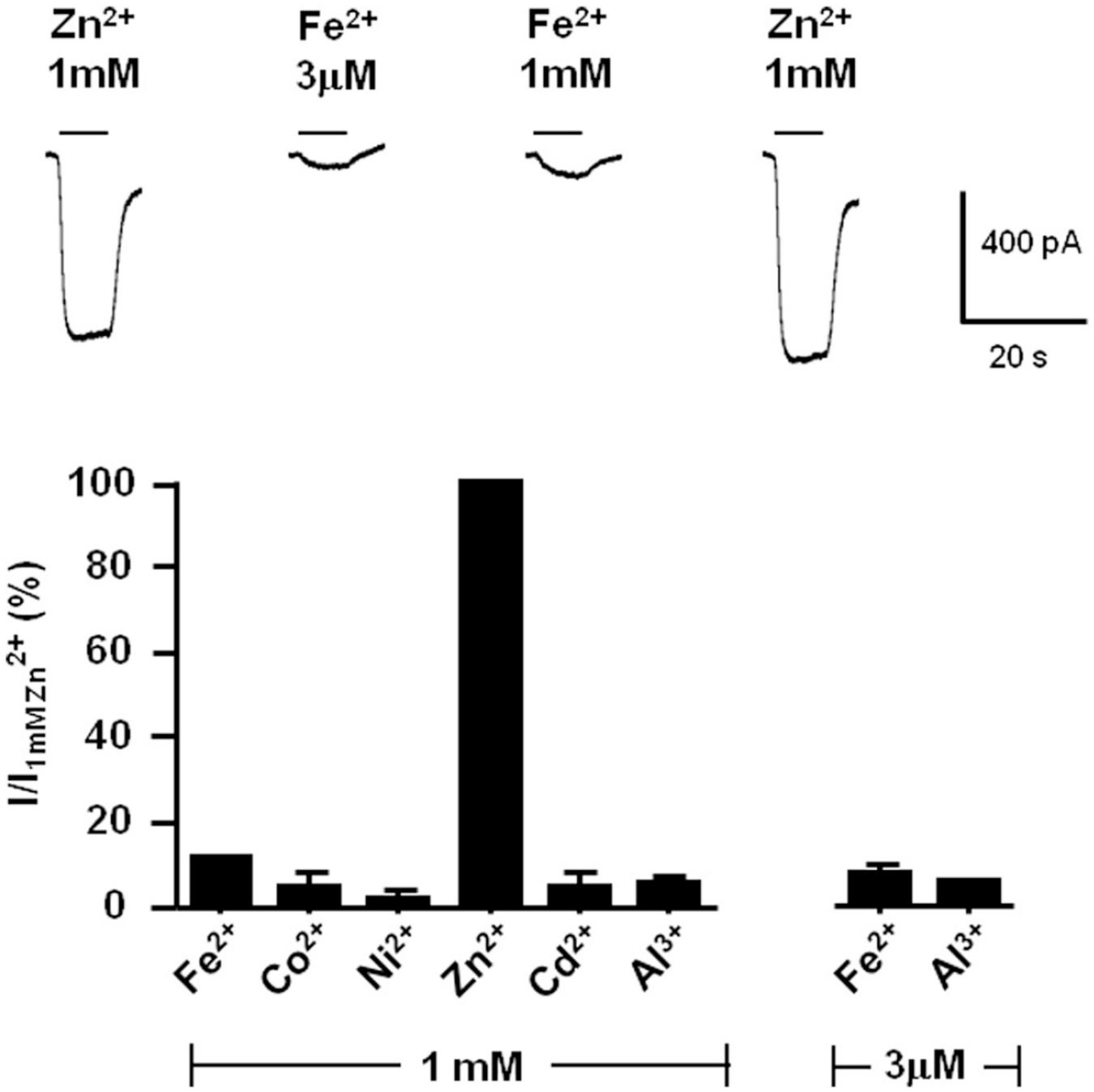

Fig. 4.

The inactivity of other metal ions at ZAC. A selection of other transition metals and aluminum are all inactive at ZAC expressed in COS-7 cells. At 1 mM concentrations, iron (Fe^{2+}), cobalt (Co^{2+}), nickel (Ni^{2+}), cadmium (Cd^{2+}), and aluminum (Al^{3+}) were either inactive or elicited negligible responses at ZAC. Zn^{2+} was used as reference agonist in the recordings.

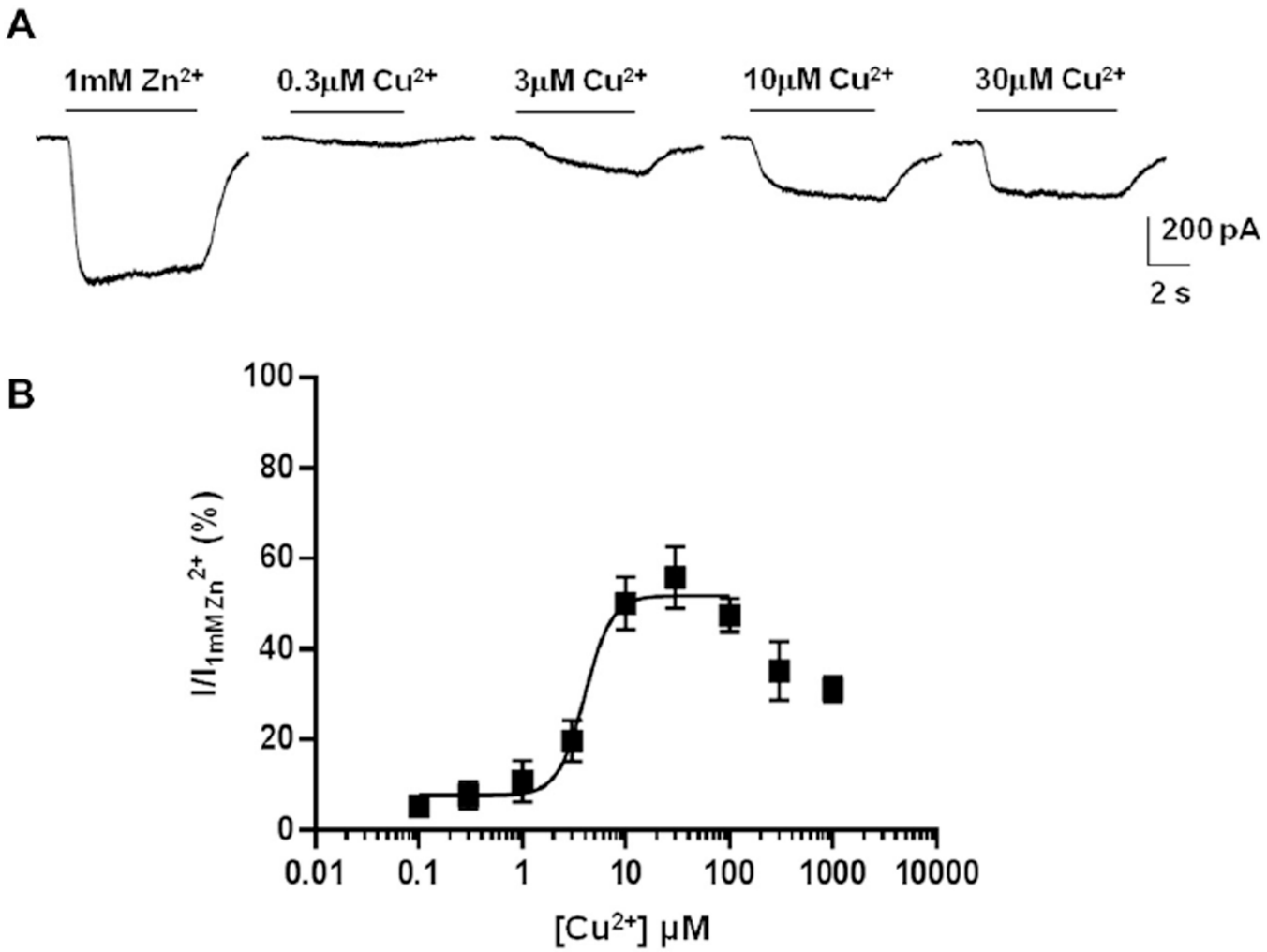

Fig. 5.

Activation of ZAC by Cu^{2+}. (A) Inward currents evoked by rapid applications of Cu^{2+} to ZAC-expressing COS-7 cells. Cu^{2+} was applied (solid bar) for 6 s to cells voltage-clamped at −60 mV and compared to currents evoked by 1 mM Zn^{2+}. (B) Cu^{2+} concentration–response relationship of ZAC relative to current evoked by 1 mM Zn^{2+}. Data shown as mean ± S.E.M. generated from 3 to 14 cells.

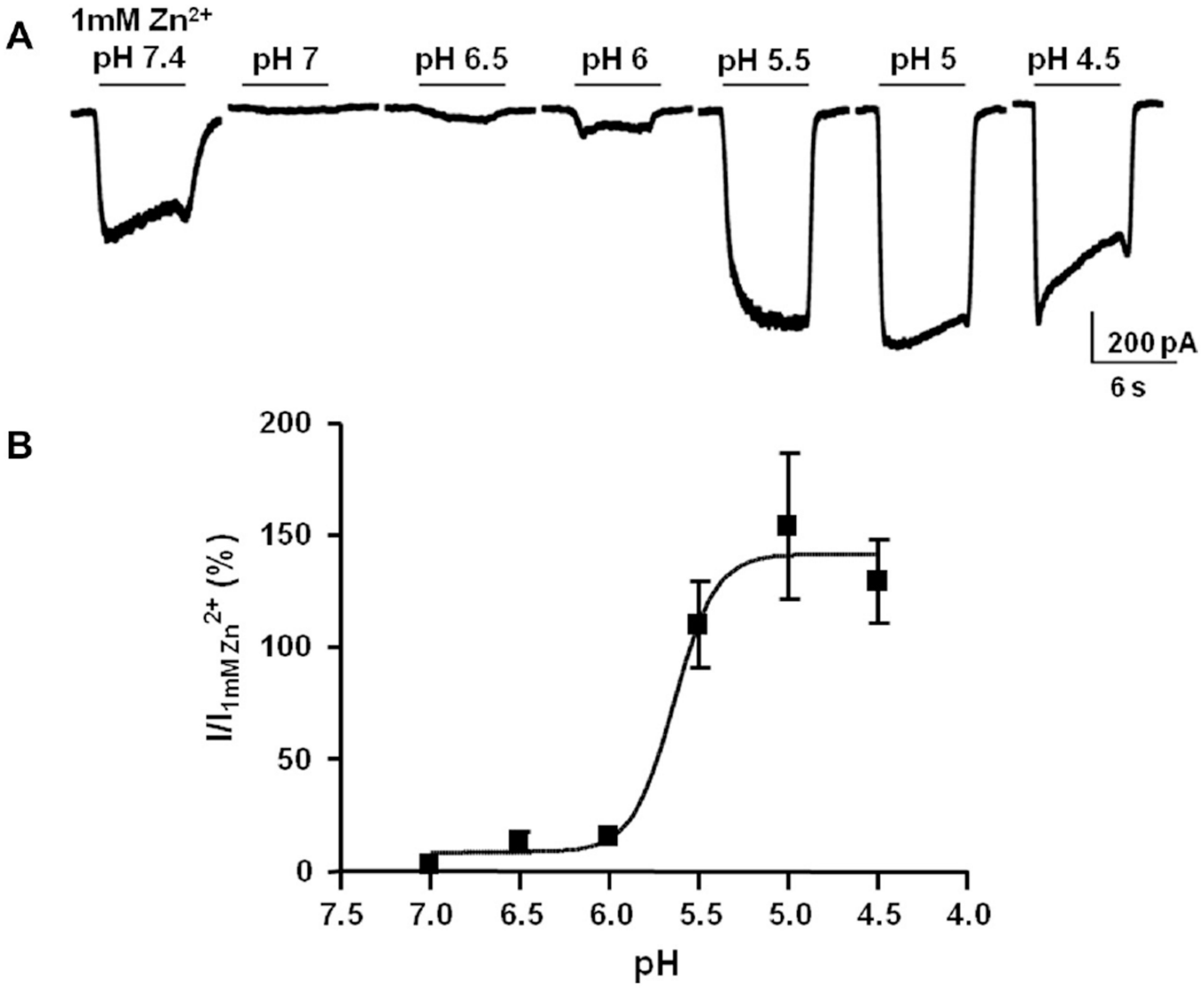

Fig. 6.

Activation of ZAC by H^+. (A) Inward currents evoked by rapid application of H^+ to ZAC-expressing COS-7 cells. Acidic extracellular solutions were rapidly applied (solid bar) for 6 s to cells voltage-clamped at −60 mV and compared to currents evoked by 1 mM Zn^{2+} (at pH 7.4). (B) H^+ concentration (pH)–response relationship of ZAC relative to current evoked by 1 mM Zn^{2+}. Data shown as mean ± S.E.M. generated from 4 to 6 cells.

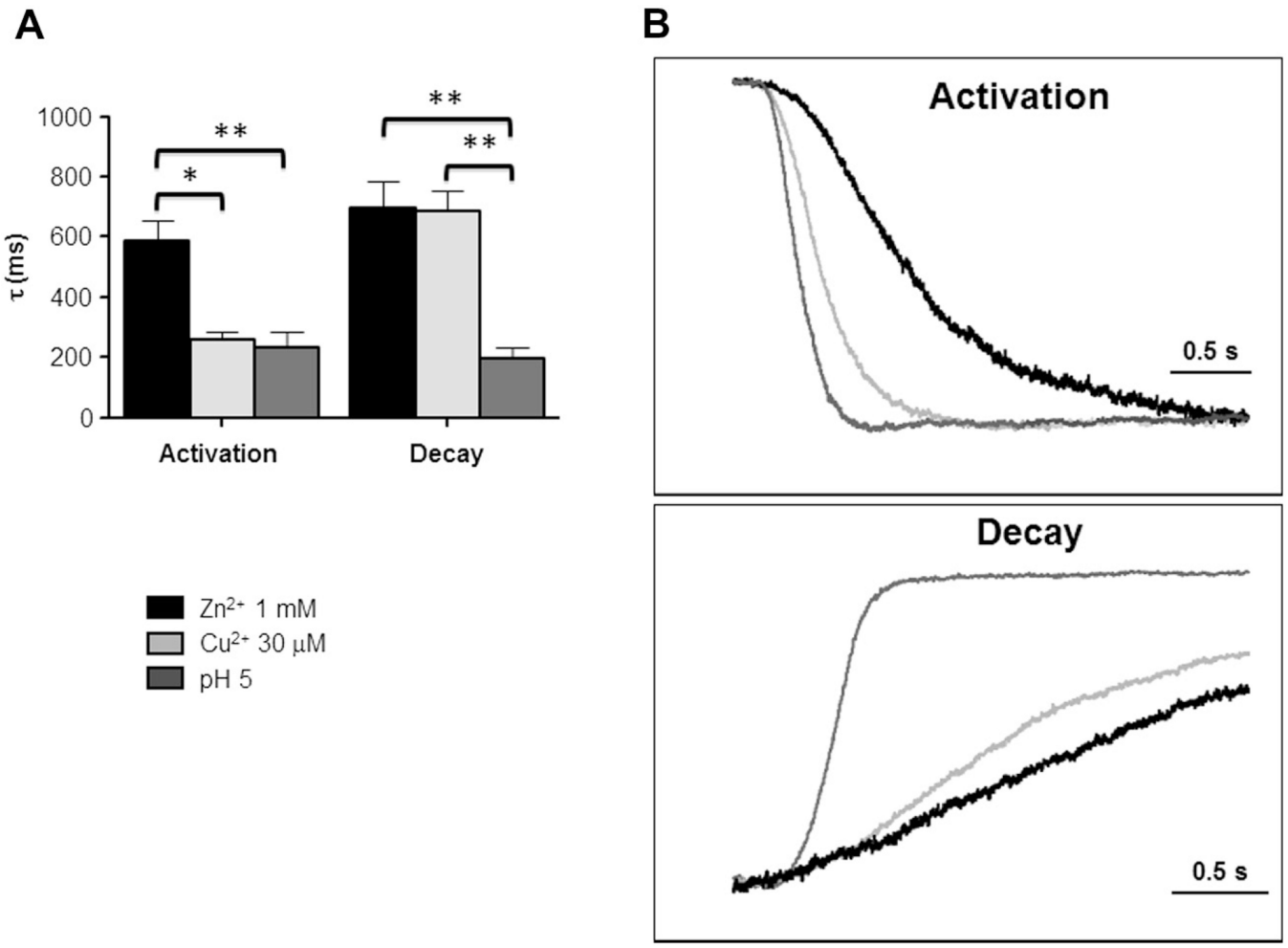

Fig. 7.

H^+-evoked currents through ZAC are characterized by faster activation and decay components than Zn^{2+}-evoked currents. (A) Time constants for activation and decay of 1 mM Zn^{2+}, 30 μM Cu^{2+}, and 10 μM H^+ (pH 5)-evoked currents. The activation phase of Zn^{2+}-evoked currents was significantly slower than Cu^{2+}- and H^+-evoked currents. Decay of H^+-evoked currents was significantly faster than Zn^{2+}- and Cu^{2+}-evoked currents. $n = 3$,* = $p < 0.05$, ** = $p < 0.01$. (B) Example current traces from independent experiments with comparable peak values for Zn^{2+}- (black), Cu^{2+}- (light gray) and H^+-evoked currents (dark gray), normalization to peak amplitudes at activation or the start of current decay, overlaid so that begin of application and wash off are in parallel for all three traces. Note the significant decay of H^+-evoked currents.

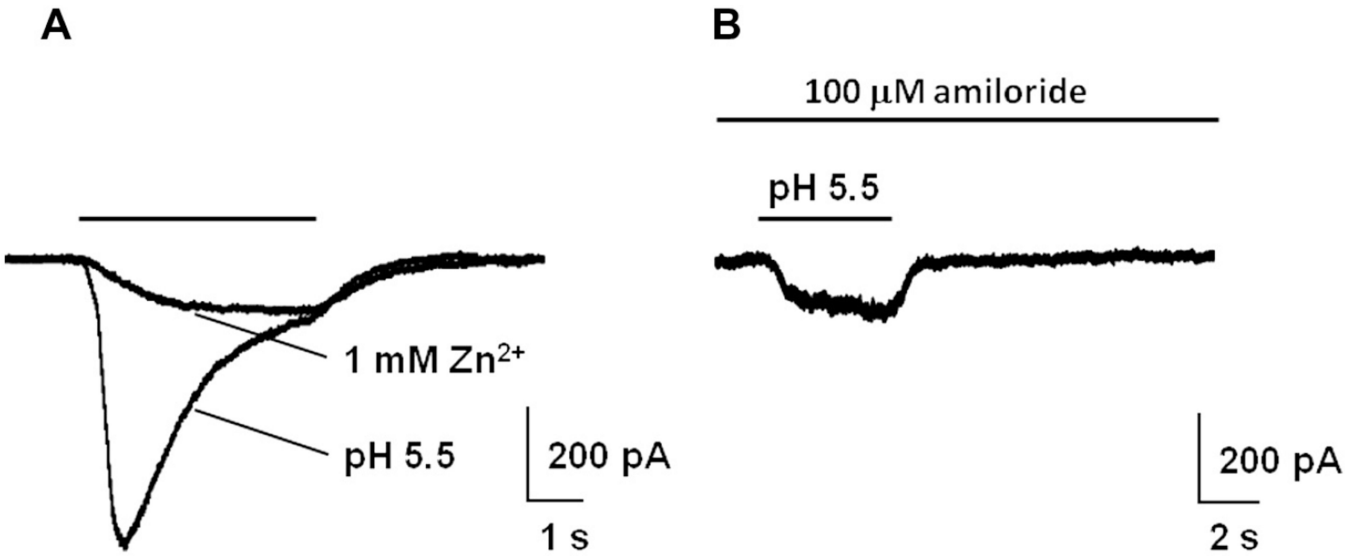

Fig. 8.

Whole-cell currents recorded from HEK293 cells expressing recombinant ZAC and endogenous ASICs. (A) Overlaid currents recorded from a HEK293 cell transfected with ZAC. Rapid application of Zn^{2+} or H^{+} (solid bar) produced different current characteristics. Zn^{2+} application produced slowly activating, non-desensitizing currents, whereas application of H^{+} produced ASIC-like faster activating currents with pronounced desensitization. (B) In the presence of amiloride, an ASIC blocker, application of H^{+} produced a typical ZAC-mediated current.

Table 1

Agonist properties at ZAC expressed in COS-7 cells.

Agonist	EC_{50} (pEC_{50} ± S.E.M.)	Hill coefficient	% Max response (of 1 mM Zn^{2+})	*n*
Zn^{2+}	180 (3.7 ± 0.02)	2.2 ± 0.2	100.1 ± 1.5	3–5
Cu^{2+}	4.0[a] (5.4 ± 0.1)	~3.3	51.8 ± 2.9	3–14
H^{+}	2.3 (5.6 ± 0.1)	3.7 ± 2.5	141.6 ± 9.8	4–6

EC_{50} values are given in μM with pEC_{50} ± S.E.M. or pH_{50} ± S.E.M. (for H^{+}) values in brackets. n refers to the number of COS-7 cells, from at least two separate transfections, used to construct the concentration–response relationships.

[a]The EC_{50} for the Cu^{2+} concentration–response curve was determined from the fit to the rising phase of the curve.